Finite Dimensional Approximation to Muscular Response in Force-Fatigue Dynamics using Functional Stimulations

Toufik Bakir, Bernard Bonnard, Sandrine Gayrard, Jérémy Rouot

Finite Dimensional Approximation to Muscular Response in Force-Fatigue Dynamics using Functional Stimulations

Toufik Bakir [a], Bernard Bonnard [b], Sandrine Gayrard [a,b], Jérémy Rouot [c]

[a] *Univ. Bourgogne Franche-Comté, ImViA Laboratory EA 7508, 9 avenue Alain Savary, Dijon, France*

[b] *INRIA, 2004 Route des Lucioles, 06902 Valbonne, France*

[c] *L@bisen, Vision-AD Team, Yncrea Ouest, 20 Rue Cuirassé Bretagne, Brest, France*

Abstract

Recent mathematical nonlinear models allow to predict the muscular response to functional electrostimulation (FES) in the isometric case or non-isometric case, based on the seminal work of V. Hill. Physical controls are Dirac pulses and this leads to a sampled-data control system, where the output is the force response. In this article, our aim is to provide a finite dimensional approximation of the force response for the non-fatigue dynamics to provide fast optimizing schemes for ongoing device, in particular the design of a smart electrostimulator for muscular reinforcement or rehabilitation or to track a reference trajectory in the non-isometric case.

Key words: Biomechanics · Force-fatigue models · Sampled-data control · Nonlinear input-output approximation · Predictive-correction methods in optimization.

1 Introduction

Recent mathematical models – based on the seminal work of V. Hill [Gesztelyi *et al.*, 2012] to analyze the muscular activity and validated experimentally – allow to predict the force response to external stimulation. They are presented and discussed in detailed in [Wilson, 2011] in the non-fatigue isometric case. They were extended in particular by Ding et al. [Ding *et al.*, 2000,Ding *et al.*, 2002a,Ding *et al.*, 2002b] to take into account the muscular fatigue and furthermore to analyze the joint variable response in the non-isometric case [Gesztelyi *et al.*, 2012]. Such models contain two basic nonlinearities, which are the nonlinear features of the response to successive pulses on the Ca^{2+}-concentration and the nonlinear dynamics relating the force response to such concentrations, modeled by the Michaelis-Menten-Hill functions. This leads to an intricate dynamics, computationally expensive due to numerical integration.

On the other hand, due to digital constraints, only a finite number of pulses can be applied over a train of electrical stimulations. From the optimal control point of view, the problem fits into the frame of optimal sampled-data control problems, studied in particular in [Bourdin & Trélat, 2016] to describe Pontryagin necessary conditions, which can be analyzed to determine optimized train pulses.

In a previous series of articles described algorithms to analyze the optimal control problems, where the controls are either the interpulse $I_i = t_i - t_{i-1}$ between two successives pulses of the amplitude of each pulses. In particular, model predictive control (MPC) methods in [Doll *et al.*, 2015] were presented and anticipate the use of online optimized

⋆ This research paper benefited from the support of the FMJH Program PGMO and from the support of EDF; Thales, Orange and the authors are partially supported by the Latex AMIES. Corresponding author J. Rouot. Email. jeremy.rouot@yncrea.fr.

Email addresses: `toufik.bakir@u-bourgogne.fr` (Toufik Bakir), `bernard.bonnard@u-bourgogne.fr` (Bernard Bonnard), `sandrine.gayrard@grenoble-inp.org` (Sandrine Gayrard), `jeremy.rouot@yncrea.fr` (Jérémy Rouot).

closed loop control scheme in the applications. Direct methods vs indirect methods based on Pontryagin type necessary conditions are discussed and numerically implemented in [Bakir *et al.*, 2019] for the isometric case or in [Bonnard & Rouot, 2020] for the non-isometric case.

This article is mainly motivated by the design of a smart electrostimulator, where the Ding et al. model is used to adjust automatically the frequency and the amplitude of the stimulations and to compute the sequence of stimulations and rest periods adapted to the task of the training program, e.g. endurance program or force maximization. Even for a single train of pulses, our previous articles using numeric integration of the dynamics lead to computational times not adapted to our task design.

Hence, the objective of this article is to propose a finite dimensional approximation of the force response, depending upon the parameters of each individual, which can be online estimated, and this allows a real time computation of the optimized amplitudes and times, for each training program.

The article is organized as follows. In section 2, the mathematical model called the Ding et al. model [Ding *et al.*, 2000,Ding *et al.*, is presented and the main properties of the dynamics are described. The section 3 presents the optimization problems, in relation with the dynamics and oriented towards the design of a smart electrostimulator. The section 4 is the core of this article, that is the construction of an integrable model for real time application. In section 5, we present some numerical stimulations aiming to validate the approximations and the optimizing scheme. In the final section 6, we present the toy application to the design of the smart electrostimulator and the path planning problem in the non-isometric case. Both are based on nonlinear output tracking, see [Hirschorn & Davis, 1987,Hirschorn & Davis, 1988] and [Isidori, 1989]. The conclusion indicates directions to complete our analysis, related to online parameters estimation of the problem [Wilson, 2011,Stein *et al.*, 2013] and MPC-methods [Richalet, 1993,Wang & Boyd, 2010] suitable for practical applications.

2 Mathematical model and main properties

We present the Ding et al. model force-fatigue model [Ding *et al.*, 2000,Ding *et al.*, 2002a,Ding *et al.*, 2002b], extension of the original Hill model [Gesztelyi *et al.*, 2012].

2.1 Ding et al. force-fatigue model [Ding et al.*, 2000,Ding* et al.*, 2002a,Ding* et al.*, 2002b]*

The FES input u over a pulse train $[0, T]$ is given by

$$u(t) = \sum_{i=0}^{n} \eta_i \delta(t - t_i), \quad t \in [0, T], \tag{1}$$

where $0 = t_0 < t_1 < \cdots < t_n < T$ are the impulsion times with $n \in \mathbb{N}$ being fixed and η_i being the amplitudes of each pulses, which are convexified by taking $\eta_i \in [0, 1]$.

Such physical control will provide the FES-signal denoted by $E(t)$, which drives the force response using electrical conduction and its dynamics is given by

$$\dot{E}(t) + \frac{E(t)}{\tau_c} = \frac{1}{\tau_c} \sum_{i=0}^{n} R_i \eta_i \delta(t - t_i), \quad a.e.\ t \in [0, T], \tag{2}$$

with $E(0) = 0$, depending upon the time response τ_c and the scaling function R_i defined by

$$R_i = \begin{cases} 1 & \text{if } i = 0 \\ 1 + (\bar{R} - 1)\, e^{-(t_i - t_{i-1})/\tau_c} & \text{otherwise}, \end{cases}$$

which codes the memory effect of successive muscle contractions and is associated to *tetanus*.

The first result is

Lemma 1 *Integrating* (2)*, one gets*

$$E(t) = \frac{1}{\tau_c} \sum_{i=0}^{n} R_i e^{-\frac{t-t_i}{\tau_c}} \eta_i H(t-t_i), \tag{3}$$

where H is the Heaviside function and the FES signal depends upon two parameters $(\tau_c, \bar{R})$.

Definition 2 *Consider a control system of the form : $\frac{\mathrm{d}x}{\mathrm{d}t} = f(x,u)$ where $x \in \mathbb{R}^n$, $u \in U \subset \mathbb{R}^m$. It is said permanent if u is a measurable bounded mapping valued in U. It is called a sampled-data control system if the set of controls is restricted to the set of piecewise constant mappings $[u_0, u_1, \ldots, u_n]$, $u_i \in U$ over a set of times $t_0 = 0 < t_1 < \cdots < t_n < T$, where n is a fixed integer.*

Our problem can be framed in the sampled-data control frame. One can write from (3),

$$E(t) = \frac{e^{-t/\tau_c}}{\tau_c} \sum_{i=0}^{n} R_i \eta_i e^{-t_i/\tau_c} H(t-t_i) = \sum_{i=0}^{n} u_i(t), \tag{4}$$

where $u_i(t)$ is the effect of the pulse $\eta_i \delta(t-t_i)$ on the linear dynamics (2). One introduces the following.

Definition 3 *For each $u_i(t)$ the restriction of u_i to $[t_i, t_{i+1}]$ is called the head and the restriction to $[t_{i+1}, T]$ is called the tail.*

Clearly the FES-input is in the generalized frame of sampled data control system, provided we take into account the time-dependence and the phenomenon of tetanus. Observe also that each impulse have an effect on the whole train $[0, T]$.

The FES signal drives the evolution of the electrical conduction according to the linear dynamics describing the evolution of Ca^{2+}-concentration c_N:

$$\dot{c}_N(t) + \frac{c_N(t)}{\tau_c} = E(t) \tag{5}$$

and integrating the (resonant) system with $c_N(0) = 0$ yields the following:

Proposition 4 *The concentration is*

$$c_N(t) = \frac{1}{\tau_c} \sum_{i=0}^{n} R_i \eta_i (t-t_i)\, e^{-\frac{t-t_i}{\tau_c}} H(t-t_i), \tag{6}$$

which are the superposition of lobes of the form

$$c_i(t) = \frac{1}{\tau_c} R_i \eta_i (t-t_i)\, e^{-\frac{t-t_i}{\tau_c}}, \tag{7}$$

whose restriction to $[t_i, t_{i+1}]$ forms the head of the corresponding lobe.

Proof 1 *Apply a time translation to the initial lobe with $R_0 = 1$.*

Introducing the functions

$$m_1(t) = \frac{c_N(t)}{K_m + c_N(t)}, \quad m_2(t) = \frac{1}{\tau_1 + \tau_2\, m_1(t)}, \tag{8}$$

where m_1 is the *Michaelis-Menten function* [Michaelis & Menten, 1913], the force response satisfies the Hill dynamics

$$\dot{F}(t) = -m_2(t)\, F(t) + m_1(t) A, \tag{9}$$

where A, K_m, τ_1, τ_2 being additional parameters and we denote by $\Lambda = (\bar{R}, \tau_c, A, K_m, \tau_1, \tau_2)$ the whole set of parameters τ_p, α_p. Using sensitivity analysis from [Bonnard & Rouot, 2020], we shall restrict our study to the case of the *force-fatigue Ding et al. model* with the single equation:

$$\dot{A}(t) = -\frac{A(t) - A_{rest}}{\tau_{fat}} + \alpha_A F(t) \tag{10}$$

for all $t \in [0, t_f]$, where t_f is the total train and $A(0) = A_{rest}$ corresponds to the fixed value of A for the non fatigue model. This leads to introduce additional parameters τ_{fat}, α_A. Typical parameters values used for numeric simulations are reported in Table A.1.

2.2 Mathematical rewriting

For the previous force-fatigue model and for the sake of the analysis, the model is rewritten as the control system

$$\dot{x}(t) = g(x(t)) + b(t) \sum_{i=0}^{n} G(t_{i-1}, t_i) H(t - t_i)\, \boldsymbol{e} \quad \text{a.e. on } [0, T] \tag{11}$$

with $x = (x_1, \ldots, x_8)^\intercal = (c_N, F, A, \bar{R}, \tau_c, \tau_1, \tau_2, K_m)^\intercal$ which splits into state variables (c_N, F, A) and fatigue parameters $\Lambda = (\bar{R}, \tau_c, \tau_1, \tau_2, K_m)$ satisfying the dynamics $\dot{\Lambda}(t) = 0$ and the system is integrated with the initial condition $x_0 = (0, 0, A_{rest}, \Lambda(0))^\intercal$ and

$$\begin{aligned} &\boldsymbol{e} = (1, 0 \ldots, 0)^\intercal, && b(t) = \tfrac{1}{\tau_c} e^{-t/\tau_c}, \\ &G(t_{i-1}, t_i) = (\bar{R} - 1) e^{t_{i-1}/\tau_c} + e^{t_i/\tau_c}, \end{aligned} \tag{12}$$

where $t_{-1} = -\infty, t_0 = 0$ and $t_{n+1} = T$.

This leads to a control system of the form

$$\dot{x}(t) = g(x(t)) + b(t) \sum_{i=0}^{n} G(t_{i-1}, t_i) \eta_i H(t - t_i)\ \boldsymbol{e} \text{ a.e. on } [0, T]$$

with $x(0) = x_0$.

The variable $\sigma = (t_1, \ldots, t_n, \eta_0, \eta_1, \ldots, \eta_n)$ belongs the finite dimensional input-space with the constraints

$$\begin{aligned} &\eta_i \in [0, 1],\ i = 0, \ldots, n \\ &0 < t_1 < \cdots < t_n < T, \quad t_i - t_{i-1} \geq I_{\min}, \quad i = 1, \ldots, n\ , \end{aligned} \tag{13}$$

where $I_{\min}$ is the smallest admissible interpulse.

Moreover the control is observed using the following observation function

$$y(t) = h(x(t)), \tag{14}$$

and $h : x \mapsto (F, A)$ serves as a direct measure of the force F and the fatigue variable A.

The following properties are straightforward but crucial in our analysis.

Proposition 5 *The input-output mapping $\sigma \mapsto y(t)$ is piecewise smooth over $[0, T]$ and smooth if $t \neq t_i,\ i = 0, \ldots, n$ (impulses times).*

Proposition 6 *For the non fatigue model, the force response can be integrated up to a time reparameterization as*

$$F(s) = \int_0^s e^{u-s} m_3(u)\,\mathrm{d}u \tag{15}$$

with

$$m_3(s) = A\frac{m_1(s)}{m_2(s)}, \quad \mathrm{d}s = m_2(t)\,\mathrm{d}t. \tag{16}$$

Proof 2 *Hill-Huxley dynamics* (9) *is rewritten as*

$$\frac{\mathrm{d}F}{\mathrm{d}s} = m_3(s) - F(s)$$

and this linear dynamics can be integrated using Lagrange formulae with $F(0) = 0$. *This proves the assertion.*

3 Optimization problems related to the design of the electrostimulator

3.1 Standard electrostimulators vs smart electrostimulators

The standard commercial electrostimulators apply a sequence of pulses trains and rest periods, where on each train $[0, T]$ the user imposes the amplitude of each impulses and this is called a CFT (constant frequency train). Our aim is to apply VFT (variable frequency trains) in order to optimize a cost related to a training program, while the rest periods have the aim to reduce the fatigue. An initial stimulation train with low amplitudes aims to scan the muscle of the user to determine the muscular parameters of the patient. If we mimic this approach, rest periods with low amplitude will allow to restimate those parameters taking into accounts the fatigue. This leads to introduce the following optimization problems associated to the design of the smart electrostimulator.

3.2 Optimization problems

3.2.1 The punch program

In this case, our aim is to optimize the force at the end of the train over each train $[0, T]$. This leads to:

OCP1: $\max_\sigma F(T)$.
In this case, the amplitude can be hold at the constant maximal amplitude $\eta = 1$ and the optimization variables are the constraint impulses times:

$$0 = t_0 < t_1 < \cdots < t_n < T.$$

Since one considers a single train, the force model is sufficient.

3.2.2 The train endurance program

We consider a single train $[0, T]$ on which the model is the force model and the corresponding problem is

OCP2: $\min_\sigma \int_0^T |F(t) - F_{ref}|^2\,\mathrm{d}t$.
Here the amplitudes are appended to the impulse times to form the optimization variables and we use the convexified amplitude constraint : $\eta_i \in [0, 1],\ i = 0, \ldots, n$.

The force reference has to be adjusted in relation with the user and can be set to $F_{\max}/k$, where k is a suitable positive number grater than 1 and $F_{\max}$ is deduced from **OCP1**.

3.2.3 The endurance program

We consider an interval $[0, t_f]$, where t_f is the total training period formed by sequences of stimulation and rest periods. In this case, one must use a force-fatigue model and we take into account the constraint $A \in [A_{rest}, A_{rest}/k'']$, where $S = A_{rest}/k''$ corresponds to a *threshold*, since as repeated in [Ding *et al.*, 2000]: if the user is exhausted, the force signal is *totally noisy*. Moreover in the case of exhaustion, a large rest period is required. This constraint can be penalized as follows

OCP3: $\min_\sigma \int_0^{t_f} |F(t) - F_{ref}|^2 \,\mathrm{d}t \, + \, w_1 \int_0^{t_f} |A(t) - A_S|^2 \,\mathrm{d}t,$
where A_S is related to S, while w_1 is a weight parameter.

4 Construction of an integrable model for real time application

4.1 Mathematical analysis of c_N

The parameter τ_c of the model is not relevant since a time reparameterization of c_N drops it according to:

$$c_N(t; t_1, \ldots, t_n, \tau_c) = c_N^\dagger \left(\frac{t}{\tau_c}; \frac{t_1}{\tau_c}, \ldots, \frac{t_n}{\tau_c} \right), \ \forall t \geq 0,$$

where $c_N(t; t_1, \ldots, t_n, \tau_c)$ is solution of (5), $c_N^\dagger(t; t_1, \ldots, t_n) = \sum_{i=0}^{n} R_i^\dagger (t - t_i)\, e^{-(t-t_i)}\, H(t - t_i)$ and

$$R_i^\dagger = \begin{cases} 1 & \text{if } i = 0 \\ 1 + (\bar{R} - 1)\, e^{-(t_i - t_{i-1})} & \text{otherwise} \end{cases}.$$

Notation 1 *A pulses train is defined by a finite sequence of impulses times $\sigma = (t_i)_{1 \leq i \leq n}$ such that $t_1 < \cdots < t_n$ and we extend it to the left by $t_0 = 0$ and to the right by $t_{n+1} = T$. In the sequel, we will prefer the notation c_N instead of $c_N^\dagger$. The restriction of c_N to $[t_k, t_{k+1}]$ is denoted as c_N^k.*

Definition 7 *A lobe at t_k is the representative curve of the function $\ell_k : \mathbb{R} \ni t \mapsto (t - t_k)\, e^{-(t-t_k)}\, H(t - t_k)$.*

Property 8 • *A lobe at t_k reaches its maximum at $t = t_k + 1$ and is equal to $1/e$. It is strictly increasing on $[t_k, t_k + 1]$ and strictly decreasing $[t_k + 1, t_{k+1}]$.*
• *There exists a unique $\iota_k \in [t_k, t_{k+1}]$ such that $\ddot{\ell}_k(\iota_k) = 0$ and therefore, ℓ_k is concave on $[t_k, \iota_k]$ and convex on $[\iota_k, t_{k+1}]$.*
• *Its function ℓ defines a density probability function and more than 95% of the values lie in $[t_k, t_k + 5]$. For all $t \geq t_k + 5$, $|\ell_k(t)| \leq 5e^{-5} \approx 0.034$.*

We introduce the notion of p-persistent pulses related to the case where $(p-1)$th successive pulses have an influence on the pth pulse.

Definition 9 *Let $t_1 < \cdots < t_p$ be p successive impulses times of a pulses train satisfying for any $i \in [\![1, p]\!]$, $t_i \leq t_{i-1} + 5$ and $t_i - t_{i-1} \geq I_{\min}$. When such integer p is maximal then the pulses train is said p-persistent.*

Remark 10 *Given an 1-persistent pulses train $(t_i)_{1 \leq i \leq n}$, there exists $j \in [\![1, n]\!]$ such that $t_j > t_{j-1} + 2$. Then, by Property 8, c_N^j is well approximated by $t \mapsto (t - t_j)\, e^{-(t-t_j)}$ for $t \in [t_j, t_{j+1}]$ (the factor $R_j^\dagger$ has a negligible effect).*

Definition 11 (Approximation of c_N.) *Let $(t_i)_{1 \leq i \leq n}$ be a 2-persistent pulses train. For $0 \leq k \leq n$, $t \in [t_k, t_{k+1}]$, we define*

$$\tilde{c}_N(t) = \begin{cases} t\, e^{-t} & \text{if } k = 0 \\ \left((t - t_{k-1})\, e^{-(t-t_{k-1})} + (t - t_k)\, e^{-(t-t_k)} \right) & \text{if } k > 0 \end{cases}. \tag{17}$$

Proposition 12 *If $(t_i)_{i=1,\dots,n}$ is at most 2-persistent then the error between c_N^k and $\tilde{c}_N^k$, $k=0,\dots,n$ is at most $5e^{-5}$. More generally, in the p-persistent case, an upper bound of this error is $\frac{p-1}{e}$.*

Proof 3 *For $1 \leq k \leq n$, for all $t \in [t_k, t_{k+1}]$, we have:*

$$c_N^k(t) = \sum_{i=0}^{k} R_i(t-t_i)e^{-(t-t_i)} \geq \sum_{i=\max(0,k-1)}^{k} (t-t_i)e^{-(t-t_i)}) = \tilde{c}_N^k$$

and

$$c_N^k(t) - \tilde{c}_N^k(t) \leq \sum_{i=0}^{k-2} (t-t_i)e^{-(t-t_i)}.$$

- *If $(t_i)_{i=1,\dots,n}$ is p-persistent, $c_N^k(t) - \tilde{c}_N^k(t) \leq \frac{p-1}{e}$ for all $t \in [t_k, t_{k+1}]$.*
- *If $(t_i)_{i=1,\dots,k-2}$ is at most 2-persistent, $t_k - t_{k-2} \geq 5$. On the other hand, for all $t \in [t_k, t_{k+1}]$ and for all $i \in \{1,\dots,k-2\}$, we have $t - t_i \geq t_k - t_i \geq t_k - t_{k-2}$. Hence $(t-t_i)e^{-(t-t_i)} \leq 5e^{-5}$ and $c_N^k(t) - \tilde{c}_N^k(t) \leq 5e^{-5}$ for all $t \in [t_k, t_{k+1}]$.*

Proposition 13 *If $(t_i)_{i=1,\dots,n}$ is p-persistent, then the error between c_N^k and $t \mapsto \sum_{i=\max(k+1-p,0)}^{k} (t-t_i)e^{-(t-t_i)}$ is at most $5e^{-5}$.*

The concentration c_N can be approximated by a piecewise constant function consisting of the averages of c_N over $[t_k, t_{k+1}]$ as described in:

Proposition 14 (Piecewise constant approximation of c_N.) *Denote for $k=0,\dots,n$, $c_N^k = c_{N|_{[t_k,t_{k+1}]}}$ and $\bar{c}_N^k = \dfrac{1}{t_{k+1}-t_k} \displaystyle\int_{t_k}^{t_{k+1}} c_N^k(t)\,\mathrm{d}t$. We have*

$$\begin{aligned} c_N^k &= \sum_{i=0}^{k} R_i\eta_i(t-t_i)e^{-(t-t_i)}, \\ \bar{c}_N^k &= \frac{1}{t_{k+1}-t_k} \sum_{i=0}^{k} R_i\eta_i \left(\chi_i(t_k) - \chi_i(t_{k+1})\right), \end{aligned} \tag{18}$$

where $\chi_i(t) = e^{-(t-t_i)}(1+t-t_i)$.

Proposition 15 (Tail approximation of c_N.) *Let $q \in \{0,\dots,n\}$. Denote the tail of c_N by $c_N^q = c_{N|_{[t_q,T]}}$ and its average over $[t_q, T]$ by $\bar{c}_N^q$. We have:*

$$\bar{c}_N^q \coloneqq \frac{1}{T-t_q}\int_{t_q}^{T} c_N^q(s)\,\mathrm{d}s = \frac{1}{T-t_q}\sum_{i=0}^{q} R_i\eta_i\left(\chi_i(t_q) - \chi_i(T)\right) + \frac{1}{T-t_q}\sum_{i=q+1}^{n} R_i\eta_i\left(1-\chi_i(T)\right), \tag{19}$$

where $\chi_i(t) = e^{-(t-t_i)}(1+t-t_i)$.

Proposition 16 *Let $t^* = \underset{t\in[t_k,t_{k+1}]}{\mathrm{argmax}}\ \tilde{c}_N^k(t)$ (or $t^* = \underset{t\in[t_k,t_{k+1}]}{\mathrm{argmax}}\ c_N^k(t)$). Then,*

- *m_1^k is strictly increasing on $[t_k, t^*]$ and strictly decreasing of $[t^*, t_{k+1}]$.*
- *m_2^k is strictly decreasing on $[t_k, t^*]$ and strictly increasing of $[t^*, t_{k+1}]$.*

The following proposition is relevant regarding the transcendence of the states c_N, F to approximate them in a stable category.

Definition 17 *The polynomial-exponential category for (piecewise) smooth functions $[0,T] \mapsto \mathbb{R}$ is the category generated by sums, products of polynomials $P(t)$ and exponential mappings to generate exponential-polynomials : $\sum_n P_n(t)e^{\lambda_n t}$. This category is stable with respect to derivation and integration.*

Using proposition 4 one has:

Lemma 18 *For $t \neq t_i$, $c_N(t)$ is in the polynomial-exponential category. Moreover, the coefficients are linear with respect to η_i and polynomial-exponential with respect to t_i.*

4.2 Approximations of F

The force, with $F(0) = 0$, is given on $[t_k, t_{k+1}]$, $k = 0, \ldots, n$, by

$$F(t) = A_0 M(t) \int_0^t M^{-1}(s) m_1(s)\, \mathrm{d}s, \tag{20}$$

where $M(t) = \exp\left(-\int_0^t m_2(s)\, \mathrm{d}s\right)$.
Consider a finer partition of $(t_i)_{1\leq i\leq n}$ denoted as $(t_{i+j/p})$, $i = 0, \ldots, n$, $j = 0, \ldots, p-1$, where $p \in \mathbb{N}^*$ and $p-1$ is the number of "new" points between t_i and t_{i+1}: $t_i < t_{i+1/p} < \cdots < t_{i+(p-1)/p} < t_{i+1}$. From (20), we construct the following approximation of F on $[t_{k+j/p}, t_{k+(j+1)/p}]$, $k = 0, \ldots, n$, $j = 0, \ldots, p-1$:

$$F(t) \approx A_0\, \tilde{M}(t) \int_0^t \tilde{M}^{-1}(s) \tilde{m}_1(s)\, \mathrm{d}s, \quad \forall t \in [t_{k+j/p}, t_{k+(j+1)/p}],$$

where $\tilde{M}(t) = \exp\left(-\int_0^t \tilde{m}_2(s)\, \mathrm{d}s\right)$, and, for $i = 1, 2$, $\tilde{m}_i$ is an approximation of m_i on $[0, T]$.

Example 19 (Triangular approximation of a lobe.) *Since $\dot{m}_1 = K_m \dot{c}_N/(K_m + c_N)^2$ and $\dot{m}_2 = \tau_2 \dot{m}_1/(\tau_1 + \tau_2 m_1)^2$, then $\dot{m}_1$, $\dot{m}_2$ are zero when c_N is maximal. On $[t_k, t_{k+(j+1)/2}]$ $j = 0, 1$, m_i, $i = 1, 2$ can be approximated by $\tilde{m}_i(t) = a_{ij,k}\,(t - t_{k+j/2}) + b_{ij,k}$, $k = 0, \ldots, n$, where $t_{k+1/2} = \underset{t\in[t_k, t_{k+1}]}{\mathit{argmax}}\ \tilde{c}_N(t)$. Computing, we have*

$$t_{1/2} = 1, \ \textit{and for } k = 1, \ldots, n, \quad t_{k+1/2} = \underset{t\in[t_k, t_{k+1}]}{\mathit{argmax}}\ \tilde{c}_N^k(t) = 1 + \frac{t_{k-1}e^{t_k - t_{k-1}} + t_k e^{t_{k+1} - t_k}}{e^{t_{k-1}} + e^{t_k}}$$

and we deduce

$$a_{ij,k} = \frac{m_i(t_{k+(j+1)/2}) - m_i(t_{k+j/2})}{t_{k+(j+1)/2} - t_{k+j/2}}, \quad b_{ij,k} = m_i(t_{k+j/2}).$$

Proposition 20 *For $k \in \{0, \ldots, n\}$, if $t_{k+1} < \iota_k$ then $m_{1|[t_k, t_{k+1}]}$ is concave and $m_{2|[t_k, t_{k+1}]}$ is convex (see Property 8 for the definition if ι_k).*

In the next paragraph, we construct approximations of m_1 and m_2, denoted as $\tilde{m}_1$ and $\tilde{m}_2$ respectively and this will yield to a closed-form expression for the force F over $[0, T]$.

Computation. Take $k_s \in \{0, \ldots, n\}$, $j_s \in \{0, \ldots, p-1\}$ and $t \in [t_{k_s+j_s/p}, t_{k_s+(j_s+1)/p}]$ and let $\Psi(u; i, j)$ be the primitive of $\tilde{m}_2$ on $[t_{i+j/p}, t_{i+(j+1)/p}]$, zero at $t = t_{i+j/p}$. We have for $t \in [t_{k_t+j_t/p}, t_{k_t+(j_t+1)/p}]$:

$$\tilde{M}(t) = \exp\left(-\sum_{k=0}^{k_s-1}\sum_{j=0}^{p-1} [\Psi(u; k, j)]_{t_{k+j/p}}^{t_{k+(j+1)/p}} - \sum_{j=0}^{j_s-1} [\Psi(u; k_s, j)]_{t_{k_s+j/p}}^{t_{k_s+(j+1)/p}} - [\Psi(u; k_s, j_s)]_{t_{k_s+j_s/p}}^{t}\right), \tag{21}$$

and for $s \in [t_{k_s+j_s/p}, t_{k_s+(j_s+1)/p}]$, $t \in [t_{k_t+j_t/p}, t_{k_t+(j_t+1)/p}]$, we get:

$$\begin{aligned}\tilde{M}(t)\tilde{M}^{-1}(s) = \exp\Bigg(&- [\Psi(u;k_s,j_s)]_s^{t_{k_s+j_s/p}} + \sum_{j=0}^{j_s-1} [\Psi(u;k_s,j)]_{t_{k_s+j/p}}^{t_{k_s+(j+1)/p}} - \sum_{j=0}^{j_t-1} [\Psi(u;k_t,j)]_{t_{k_t+j/p}}^{t_{k_t+(j+1)/p}} \\ &- \sum_{i=k_s}^{k_t-1}\sum_{j=0}^{p-1} [\Psi(u;i,j)]_{t_{i+j/p}}^{t_{i+(j+1)/p}} - [\Psi(u;k_t,j_t)]_{t_{k_t+j_t/p}}^{t} \Bigg).\end{aligned} \tag{22}$$

To integrate the product $\tilde{M}(t)\tilde{M}^{-1}(s)\tilde{m}_1(s)$ with respect to s, we gather the terms depending on s in (22) together and we get, for $t \in [t_{k_t+j_t/p}, t_{k_t+(j_t+1)/p}]$:

$$\begin{aligned}&\int_{t_{k_s+j_s/p}}^{t_{k_s+(j_s+1)/p}} \tilde{M}(t)\tilde{M}^{-1}(s)\,\tilde{m}_1(s)\,\mathrm{d}s = \int_{t_{k_s+j_s/p}}^{t_{k_s+(j_s+1)/p}} \exp\left(\Psi(s;k_s,j_s)\right)\ \tilde{m}_1(s)\,\mathrm{d}s \\ &\exp\Bigg(- \Psi(t;k_t,j_t) + \sum_{j=0}^{j_s-1} \Psi(t_{k_s+(j+1)/p};k_s,j) - \sum_{j=0}^{j_t-1} \Psi(t_{k_t+(j+1)/p};k_t,j) - \sum_{i=k_s}^{k_t-1}\sum_{j=0}^{p-1} \Psi(t_{i+(j+1)/p};i,j)\Bigg).\end{aligned} \tag{23}$$

Consequently, we obtain an approximation of F on $[t_{k_t+j_t/p}, t_{k_t+(j_t+1)/p}]$, $k_t = 0,\dots,n$, $j_t = 0,\dots,p-1$ writing:

$$\begin{aligned}\tilde{F}(t)/A0 &= \int_0^t \tilde{M}(t)\tilde{M}^{-1}(s)\,\tilde{m}_1(s)\,\mathrm{d}s \\ &= \sum_{i=0}^{k_t-1}\sum_{j=0}^{p-1} \int_{t_{i+j/p}}^{t_{i+(j+1)/p}} \tilde{M}(t)\tilde{M}^{-1}(s)\,\tilde{m}_1(s)\,\mathrm{d}s + \sum_{j=0}^{j_t-1} \int_{t_{k_t+j/p}}^{t_{k_t+(j+1)/p}} \tilde{M}(t)\tilde{M}^{-1}(s)\,\tilde{m}_1(s)\,\mathrm{d}s \\ &+ \int_{t_{k_t+j_t/p}}^{t} \tilde{M}(t)\tilde{M}^{-1}(s)\,\tilde{m}_1(s)\,\mathrm{d}s.\end{aligned} \tag{24}$$

Remark 21 *In these computations, the functions m_1 and m_2 are considered independently in the sense that this method does not rely on the relation between m_1 and m_2 (see (8)). A direct consequence is that an upper approximation of the force can be obtained from an upper approximation of m_1. Outside the scope of this paper, this method may be applied for more general non-autonomous models.*

Proposition 22 *Adding a real parameter to the functions $\tilde{m}_1, \tilde{m}_2$ as in the functions*

$$\breve{\tilde{m}}_1(t;k) = \frac{c_N(t)}{k\,K_m + c_N(t)} \ \textit{and}\ \breve{\tilde{m}}_2(t;k) = \frac{k}{\tau_1 + \tau_2\,m_1(t)} \tag{25}$$

allows to construct an upper (or lower) approximation $\tilde{F}$ of F parameterized by k.

Error estimate.

The following proposition gives an estimate of the error between the approximation $\tilde{F}$ and F in the case where $\tilde{m}_2^k$ is the average of m_2 on $[t_k, t_{k+1}]$.

Proposition 23 (Piecewise constant approximation of m_2.) *Consider the case where $0 \le \tilde{m}_1(t) \le 1$ and $\tilde{m}_2$ is equal to the average of m_2 on $[t_j, t_{j+1}]$, $j = 0,\dots,n$. Assume moreover that each restriction on $[t_j, t_{j+1}]$, $j = 0,\dots,n$ of m_1 (resp. m_2) is concave (resp. convex). Then, the error between the force F and its the approximation $\tilde{F}$ defined by (24) satisfies for $k = 0,\dots,n$:*

$$|F(t_k) - \tilde{F}(t_k)|/A_0 \le \int_0^{t_k} |m_1(s) - \tilde{m}_1(s)|\,\mathrm{d}s + T\int_0^{t_k} |m_2(s) - \tilde{m}_2(s)|\,\mathrm{d}s.$$

Proof 4 *For $t_k > s$, we have:*

$$
\begin{aligned}
|F(t_k) - \tilde{F}(t_k)|/A_0 &= \left| \int_0^{t_k} M(t_k)M^{-1}(s)m_1(s) - \tilde{M}(t_k)\tilde{M}^{-1}(s)\tilde{m}_1(s)\,\mathrm{d}s \right| \\
&\leq \int_0^{t_k} M(t_k)M^{-1}(s)|m_1(s) - \tilde{m}_1(s)|\,\mathrm{d}s + \left| \int_0^{t_k} \tilde{m}_1(s)M(t_k)M^{-1}(s) - \tilde{M}(t_k)\tilde{M}^{-1}(s)|\,\mathrm{d}s \right| \\
&\leq \int_0^{t_k} |m_1(s) - \tilde{m}_1(s)|\,\mathrm{d}s + \left| \int_0^{t_k} M(t_k)M^{-1}(s) - \tilde{M}(t_k)\tilde{M}^{-1}(s)\,\mathrm{d}s \right|. \\
&= \int_0^{t_k} |m_1(s) - \tilde{m}_1(s)|\,\mathrm{d}s + \left| \int_0^{t_k} \exp\left(-\int_s^{t_k} m_2(u)\,\mathrm{d}u \right) - \exp\left(-\int_s^{t_k} \tilde{m}_2(u)\,\mathrm{d}u \right)\,\mathrm{d}s \right| \\
&= \int_0^{t_k} |m_1(s) - \tilde{m}_1(s)|\,\mathrm{d}s + \left| \sum_{i=0}^{k-1} \int_{t_i}^{t_{i+1}} \exp\left(-\int_s^{t_k} m_2(u)\,\mathrm{d}u \right) - \exp\left(-\int_s^{t_k} \tilde{m}_2(u)\,\mathrm{d}u \right)\,\mathrm{d}s \right|.
\end{aligned}
$$

Recall the function m_2 is decreasing on $[t_i, s_i]$ and increasing on $[s_i, t_{i+1}]$ where s_i is the unique maximum of c_N on $[t_i, t_{i+1}]$. Define $\xi(s) \coloneqq \tilde{m}_2(s) - m_2(s)$. Since m_2 is convex on $[t_i, t_{i+1}]$, we have three cases:

(i) $\int_{t_i}^{s} \xi(u)\,\mathrm{d}u \leq 0$ *for* $s \in [t_i, t_{i+1}]$. *We have, for* $i = 0, \ldots, k-1$,

$$
\begin{aligned}
&\left| \int_{t_i}^{t_{i+1}} \exp\left(-\int_s^{t_k} m_2(u)\,\mathrm{d}u \right) - \exp\left(-\int_s^{t_k} \tilde{m}_2(u)\,\mathrm{d}u \right)\,\mathrm{d}s \right| \\
&\qquad = \left| \int_{t_i}^{t_{i+1}} \exp\left(\int_{t_k}^{s} m_2(u)\,\mathrm{d}u \right) \left(1 - \exp\left(\int_{t_k}^{s} \xi(u)\,\mathrm{d}u \right) \right)\,\mathrm{d}s \right| \\
&\qquad \leq \int_{t_i}^{t_{i+1}} \left| 1 - \exp\left(\int_{t_i}^{s} \xi(u)\,\mathrm{d}u \right) \right| \mathrm{d}s, \ \textit{(since } \int_{t_j}^{t_{j+1}} \xi(u)\,\mathrm{d}u = 0) \\
&\qquad \leq \int_{t_i}^{t_{i+1}} \int_{t_i}^{s} -\xi(u)\,\mathrm{d}u\,\mathrm{d}s \\
&\qquad \leq (t_{i+1} - t_i) \int_{t_i}^{t_{i+1}} |\xi(u)|\,\mathrm{d}u.
\end{aligned}
\tag{26}
$$

(ii) $\int_{t_i}^{s} \xi(u)\,\mathrm{d}u \geq 0$ *for* $s \in [t_i, t_{i+1}]$. *We obtain the same inequality as in the case (i) by replacing* ξ *by* $-\xi$.

(iii) There exists an unique $\theta_i \in [t_i, t_{i+1}]$ *such that* $\int_{t_i}^{s} \xi(u)\,\mathrm{d}u \leq 0$ *for* $s \in [t_i, \theta_i]$ *and* ≥ 0 *for* $s \in [\theta_i, t_{i+1}]$. *Write*

$$
\begin{aligned}
&\left| \int_{t_i}^{t_{i+1}} \exp\left(-\int_s^{t_k} m_2(u)\,\mathrm{d}u \right) - \exp\left(-\int_s^{t_k} \tilde{m}_2(u)\,\mathrm{d}u \right)\,\mathrm{d}s \right| \\
&\qquad \leq \left| \int_{t_i}^{\theta_i} \exp\left(-\int_s^{t_k} m_2(u)\,\mathrm{d}u \right) - \exp\left(-\int_s^{t_k} \tilde{m}_2(u)\,\mathrm{d}u \right)\,\mathrm{d}s \right| \\
&\qquad\qquad + \left| \int_{\theta_i}^{t_{i+1}} \exp\left(-\int_s^{t_k} m_2(u)\,\mathrm{d}u \right) - \exp\left(-\int_s^{t_k} \tilde{m}_2(u)\,\mathrm{d}u \right)\,\mathrm{d}s \right|
\end{aligned}
\tag{27}
$$

We have: $\int_{\theta_i}^{s} \xi(u)\,\mathrm{d}u \leq 0$ *for* $s \in [t_i, \theta_i]$ *and* ≥ 0 *for* $s \in [\theta_i, t_{i+1}]$. *As in the case (i), the first integral in the right hand side of* (27) *is bounded by* $(\theta_i - t_i) \int_{t_i}^{\theta_i} |\xi(u)|\,\mathrm{d}u$. *Likewise, the second integral in the right hand side of* (27) *is bounded by* $(t_{i+1} - \theta_i) \int_{\theta_i}^{t_{i+1}} |\xi(u)|\,\mathrm{d}u$.

Finally, we obtain that in all these three cases,

$$\left| \int_{t_i}^{t_{i+1}} \exp\left(- \int_s^{t_k} m_2(u)\,\mathrm{d}u \right) - \exp\left(- \int_s^{t_k} \tilde{m}_2(u)\,\mathrm{d}u \right)\,\mathrm{d}s \right| \leq T \int_{t_i}^{t_{i+1}} |\xi(u)|\,\mathrm{d}u,$$

and it concludes the proof.

5 Numerical solution to optimization problems

We recall basic facts about finite dimensional optimization, see [Boyd & Vandenberghe, 2004] for details, to emphasize that an optimal sampled-data control problem can be viewed as an instance of such optimization problem. The aim is to compute a local minimum $\sigma^* = (\eta_0^*, \ldots, \eta_n^*, t_1^*, \ldots, t_n^*) \in \mathbb{R}_+^{2n+1}$ of a cost function denoted as Θ. For a practical implementation, this minimum have to be computed efficiently (real time computation).

The optimization problems, associated to the optimal sampled-data control problems **OCP1** and **OCP2** presented in Section 3.2, can be written in the form:

$$\begin{aligned} \min_{\sigma}\ & \Theta(\sigma) \\ & \Im(\sigma) \leq 0, \end{aligned} \tag{28}$$

where $\Im(\sigma) = (\Xi_1(\sigma), \ldots, \Xi_{3n+5}(\sigma))$ is the vector of constraints defined by:

$$\begin{aligned} &\Xi_i(\sigma^*) = t_{i-1}^* - t_i^* + I_m,\ i = 1, \ldots n, \\ &\Xi_{n+1}(\sigma^*) = t_n^* - T, \\ &\Xi_{n+2+i}(\sigma^*) = -\eta_i^*,\ i = 0, \ldots n+1, \\ &\Xi_{2n+4+i}(\sigma^*) = \eta_i^* - 1,\ i = 0, \ldots n+1. \end{aligned}$$

The map $\Theta : \sigma \mapsto \Theta(T)$ is smooth with respect to σ whenever $t \neq t_i$.
Consider the Lagrangian defined for all $(\sigma, \mu) \in \mathbb{R}^{2n+1} \times {\mathbb{R}_+}^{3n+5}$ by:

$$\mathcal{L}(\sigma, \mu) = \Theta(\sigma) + \mu \cdot \Im(\sigma).$$

The problem 28 is equivalent to the primal problem

$$\inf_{\sigma \in \mathbb{R}^{2n+1}} \sup_{\mu \in {\mathbb{R}_+}^{3n+5}} \mathcal{L}(\sigma, \mu)$$

and the first order necessary optimality conditions for σ^* to be a local minimizer, assuming the vectors $\Xi_i'(\sigma^*),\ i \in \{i,\ \Xi_i(\sigma^*) = 0\}$ to be linearly independent, state that there exists a Lagrange multiplier $\lambda \in \mathbb{R}^{3n+5}$ such that

$$\Theta'(\sigma^*) + \lambda \cdot \Im(\sigma^*) = 0, \quad \lambda_i \geq 0,\ \Xi_i(\sigma^*) \leq 0, \quad \lambda \cdot \Im(\sigma) = 0.$$

We usually do not solve directly these optimality conditions to compute an optimal pair (σ^*, μ^*), but a relaxation of these conditions can lead to efficient algorithm, namely the primal-dual interior point method [Boyd & Vandenberghe, 2004].

We present next the use of this algorithm for different costs and validate it for its use in real time application. The real time requirement prevents us (at least when Θ involves the force) from using direct or indirect methods such as those presented in [Bakir *et al.*, 2020], mainly because these methods require a numerical scheme to approximate the variable F.

We run an interior point method on a standard computer [1] to solve the optimization problem (28) using the approximations of the variable c_N and F described in the previous section. For $n \simeq 10$, $p \simeq 2$, the approximation $\tilde{\Theta}$ consists in millions of bytes, it is then crucial to use an approximation of the gradient of $\tilde{\Theta}$, with respect to $t_i,\ i = 1, \ldots, n$, via finite differences (vs formal computation). We initialize the pulses train to a regular partition of $[0, 1]$ and the initial amplitudes are equal to 1 .

[1] 4 Intel@Core^{TM} i5 CPU @ 2.4Ghz

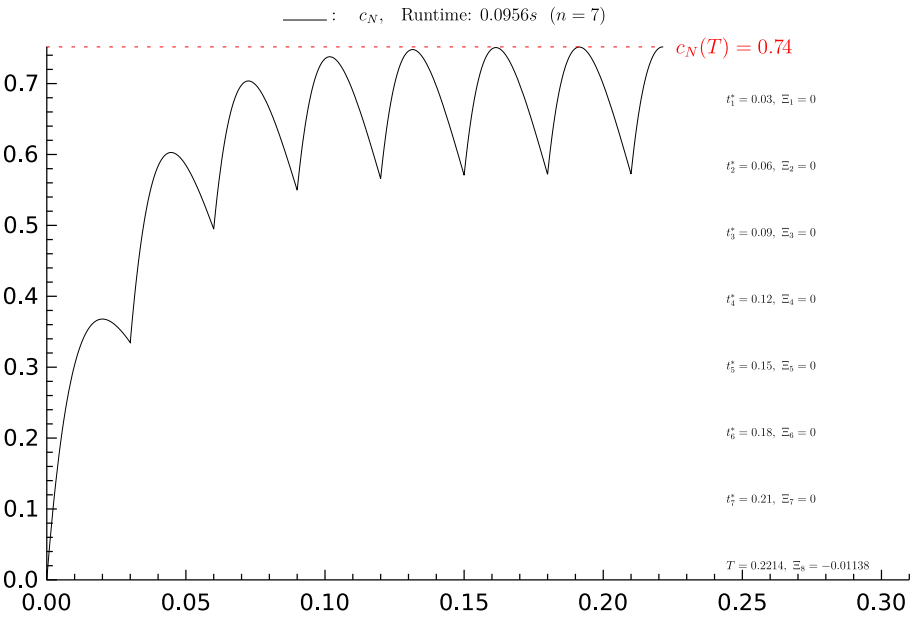

Fig. 1. Time evolution of c_N associated to the optimal sampling times σ^* for $\max_\sigma c_N(T)$ (T free) under the constraints $\Xi_i \leq 0,\ i = 1, \ldots, n+1$ (see (28)). Values of the constants are $\tau_c = 20$ms, $n = 7$, $I_m = 20$ms. The algorithm converges in less than 1s.

5.1 Ca^{2+} concentration optimization

5.1.1 Problem 1: $\Theta(\sigma) = -c_N(T)$.

True cost. We have an explicit expression for c_N, this problem can be easily solved numerically. We consider the finite dimensional optimization problem 28 where the cost is

$$\Theta(\sigma) = \sum_{i=0}^{n} R_i(T - t_i)\, e^{-\frac{T-t_i}{\tau_c}}.$$

(Note that the amplitudes are fixed to 1).

Numerical result: Fig. 1 represents the time evolution of c_N associated to (locally) optimal impulse times.

5.1.2 Problem 2: $\Theta(\sigma) = \int_0^T |c_N(t) - c_{ref}|^2 \,\mathrm{d}t$, T free.

In this case, we approximate Θ by

$$\tilde{\Theta}(\sigma) = \sum_{k=0}^{n} \left(\tilde{c}_N(t_{k+1}) - c_{ref}\right)^2 \ (t_{k+1} - t_k), \tag{29}$$

where the amplitudes and T are free and $\tilde{c}_N$ is given by (17).

Numerical result: The optimal solution σ^* and its response c_N are depicted in Fig. 2.

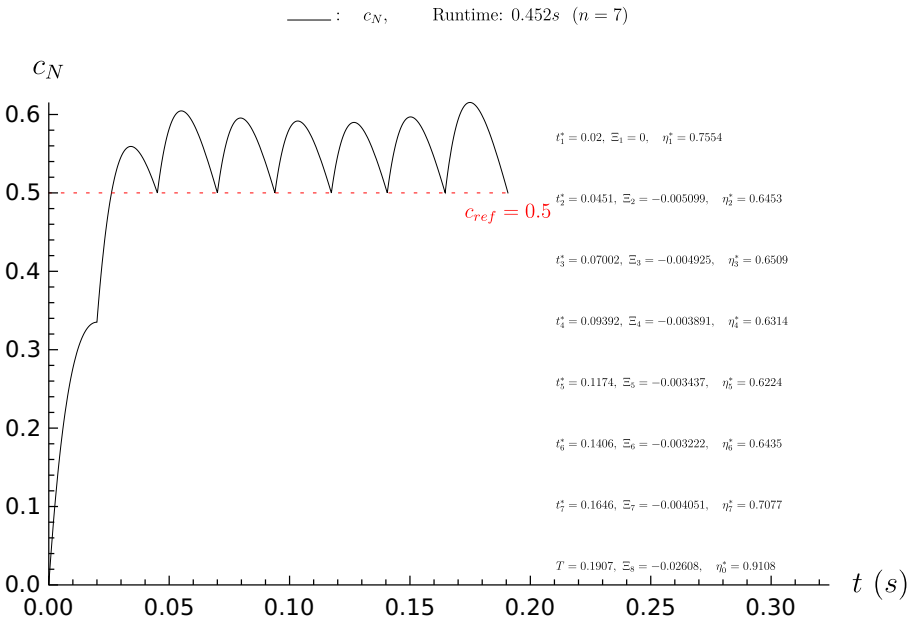

Fig. 2. The dashed curve is the time evolution of c_N associated to the optimal solution $\sigma^* = (\eta_0^*, \ldots, \eta_n^*, t_1^*, \ldots, t_n^*)$ of $\min_\sigma \sum_{k=0}^n \left(\tilde{c}_N^k(t_{k+1}) - c_{ref}\right)^2 (t_{k+1} - t_k)$ (T free), where $\tilde{c}_N$ is defined by (17), under the constraints $\Xi_i \leq 0,\ i = 1, \ldots, 3n+5$ (see (28)). The continuous curve is the response $t \mapsto c_N(t)$ to σ^*. Constants for these simulations are $\tau_c = 20$ms, $n = 7$, $I_m = 20$ms and $c_{ref} = 0.5$.

5.2 Force optimization

We consider the force approximation $\tilde{F}$ defined by (24) taking the piecewise affine functions $\tilde{m}_1, \tilde{m}_2$ to be equal on $[t_k, t_{k+1}]$, $k = 0, \ldots, n$ to

$$\tilde{m}_1(t) = \begin{cases} m_1(t_{k+1/2}) & \text{if } t \in [t_k, t_{k+1/2}] \\ a_{1j,k}\,(t - t_k) + b_{1j,k}, & \text{if } t \in [t_{k+1/2}, t_{k+1}] \end{cases}, \quad \tilde{m}_2(t) = \begin{cases} \frac{m_2(t_k) + m_2(t_{k+1/2})}{2} & \text{if } t \in [t_k, t_{k+1/2}] \\ \frac{m_2(t_{k+1/2}) + m_2(t_{k+1})}{2}, & \text{if } t \in [t_{k+1/2}, t_{k+1}] \end{cases}, \quad (30)$$

where $t_{k+1/2} = \underset{u \in [t_k, t_{k+1}]}{\operatorname{argmax}}\ m_1(u)$, $a_{1j,k} = (m_1(t_{k+1}) - m_1(t_{k+1/2}))/(t_{k+1} - t_{k+1/2})$ and $b_{1j,k} = m_1(t_{k+1/2})$.

5.2.1 Problem 3: $\Theta(\sigma) = -F(T)$ (T free).

Approximated cost. The objective function $\Theta(\sigma) = -F(T)$ is approximated by the function $\tilde{\Theta}(\sigma) = -\tilde{F}(T)$. The optimization variables consist in the impulse times while the amplitudes are fixed to 1.

Numerical result: The optimal solution σ^* and the force response F are depicted in Fig. 3.

5.2.2 Problem 4: $\Theta(\sigma) = \int_0^T |F(t) - F_{ref}|^2\,\mathrm{d}t$ (T free).

The cost $\Theta(\sigma) = \int_0^T |F(s) - F_{ref}|^2\,\mathrm{d}s$ is approximated by :

$$\tilde{\Theta}(\sigma) = \sum_{k=0}^{n} \left(\tilde{F}(t_{k+1}) - F_{ref}\right)^2,$$

where the approximated force $\tilde{F}$ is defined from (2) and the function $\tilde{m}_1$ and $\tilde{m}_2$ are replaced by approximations of the functions of $\breve{\tilde{m}}_1(t; 0.95)$ and $\breve{\tilde{m}}_2(t; 0.9)$ respectively – defined in Proposition 22.

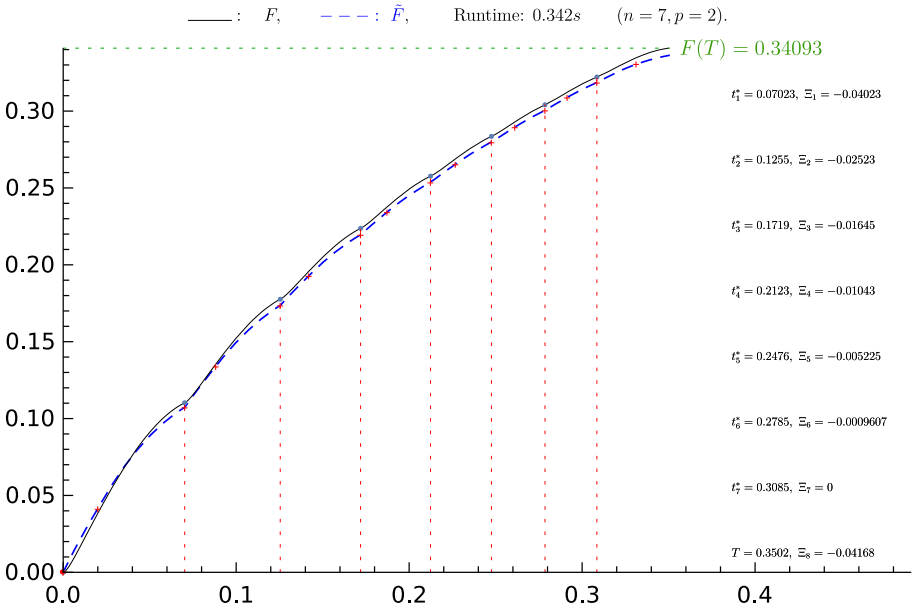

Fig. 3. The dashed curve is the time evolution of F associated to the optimal solution $\sigma^* = (t_1^*, \ldots, t_n^*)$ of $\max_\sigma \tilde{F}^n(T)$ (T free) (see (24) for the definition of $\tilde{F}$) under the constraints $\Xi_i \leq 0,\ i = 1, \ldots, n+1$ (see (28)). The continuous curve is the response $t \mapsto F(t)$ to σ^*. Values of the constants are $\tau_c = 20$ms, $n = 7$, $I_m = 20$ms.

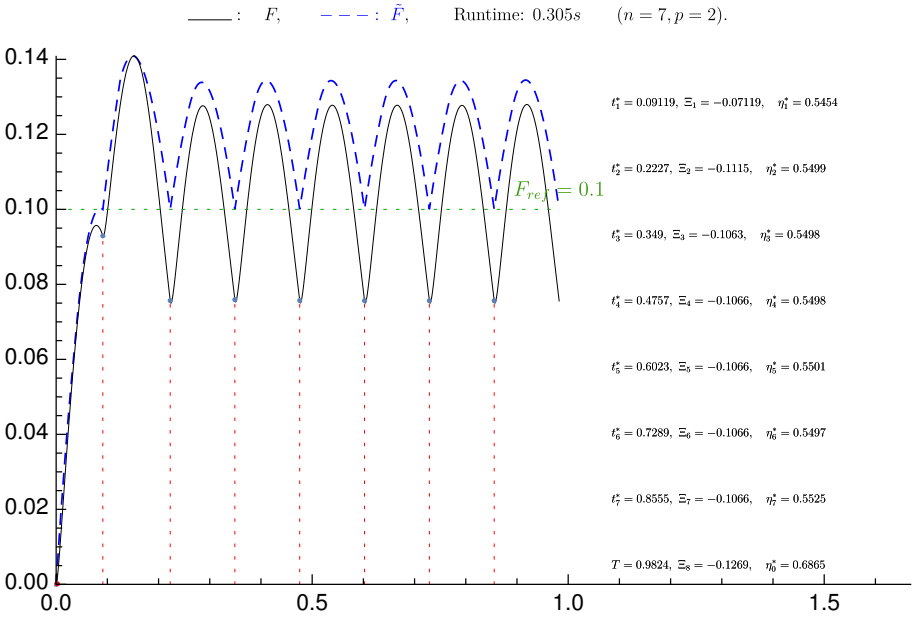

Fig. 4. The dashed curve is associated to the optimal solution $\sigma^* = (\eta_0^*, \ldots, \eta_n^*, t_1^*, \ldots, t_n^*)$ of $\min_\sigma \sum_{k=0}^n \left(\tilde{F}(t_{k+1}) - F_{ref}\right)^2 (t_{k+1} - t_k)$ ($T = t_{n+1}$ is free), where $\tilde{F}$ is the approximated force given by (24), under the constraints $\Xi_i \leq 0,\ i = 1, \ldots, 3n+5$ (see (28)). The continuous curve is the response $t \mapsto F(t)$ to σ^*. Values of the constants are $\tau_c = 20$ms, $n = 5$, $I_m = 20$ms and $F_{ref} = 0.1$kN.

Numerical result: The optimal solution σ^* and the force response F are depicted in Fig. 4-5.

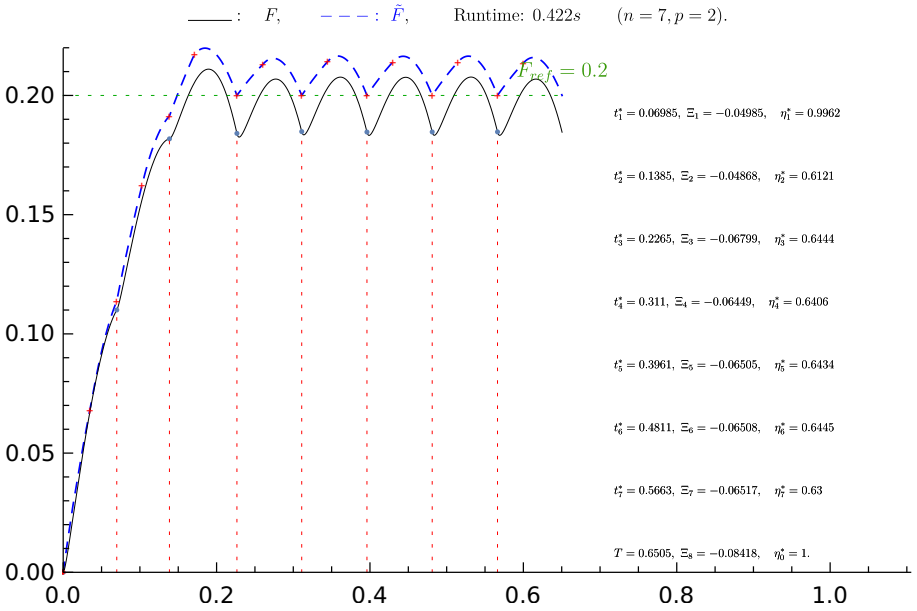

Fig. 5. The dashed curve is associated to the optimal solution $\sigma^* = (\eta_0^*, \ldots, \eta_n^*, t_1^*, \ldots, t_n^*)$ of $\min_\sigma \sum_{k=0}^n \left(\tilde{F}(t_{k+1}) - F_{ref}\right)^2 (t_{k+1} - t_k)$ ($T = t_{n+1}$ is free), where $\tilde{F}$ is the approximated force given by (24), under the constraints $\Xi_i \leq 0,\ i = 1, \ldots, 3n + 5$ (see (28)). The continuous curve is the response $t \mapsto F(t)$ to σ^*. Values of the constants are $\tau_c = 20$ms, $n = 7$, $I_m = 20$ms and $F_{ref} = 0.2$kN.

6 Two cases studies based on the approximation

In this section we apply our framework to analyze two cases studies related to ongoing works. It concerns the isometric and non-isometric case, and are associated to (sub-optimal) motion planning, see [Hirschorn & Davis, 1987,Hirschorn & Davis, 19 for the theoretical foundations.

6.1 Isometric case : design of a smart muscular electrostimulator

Advanced commercial muscular electrostimulator for training or reeducation purposes are based on the following. First of all, the user is defining a program training. Basically endurance program with low frequency sequences of trains (with constant interpulse) or force strengthening with high frequency trains. The program is a sequence of trains or rest periods. Before starting, the muscle is scanned to determine the parameters. A smart electrostimulator based on our study aims to design automatically such sequence, each program being translated into an optimization problem. Besides, in our framework, one can used VFT (Variable Frequency Trains) or CFT (Constant Frequency trains) in the standard case to complete the tuning of the amplitude.

One needs the following proposition associated to the endurance program presented in figure 6 to illustrate the smart electrostimulator conception.

Proposition 24 *Consider the reference program, where a reference force F_{ref} is given. Plugging such F_{ref} in $\dot{F} = 0$ leads to solve the equation : $A\tau_2 m_1^2 + A\tau_1 m_1 - F_{ref} = 0$ which has one unique positive root m_1^+, which gives the reference concentration C_{Nref}. This root is stable and leads to design an optimized pulse train solving the L^2-optimization problem : $\displaystyle\int_0^T |c_N(t) - c_{N,ref}|^2 \, \mathrm{d}t$.*

Proof 5 *Note that the mapping $m_1 : c_N \mapsto m_1(c_N)$ is one-to-one and m_1 can be taken as an accessory control in place of c_N. Solving in m_1 the equation $\dot{F} = 0$ leads to real roots denoted respectively $m_1^+ > 0$ and $m_1^- < 0$. Taking m_1^+, stability is granted since $\lambda = -m_2(c_N^+)$ is negative, where c_N^+ is given by $m_1(c_N^+) = m_1^+$.*

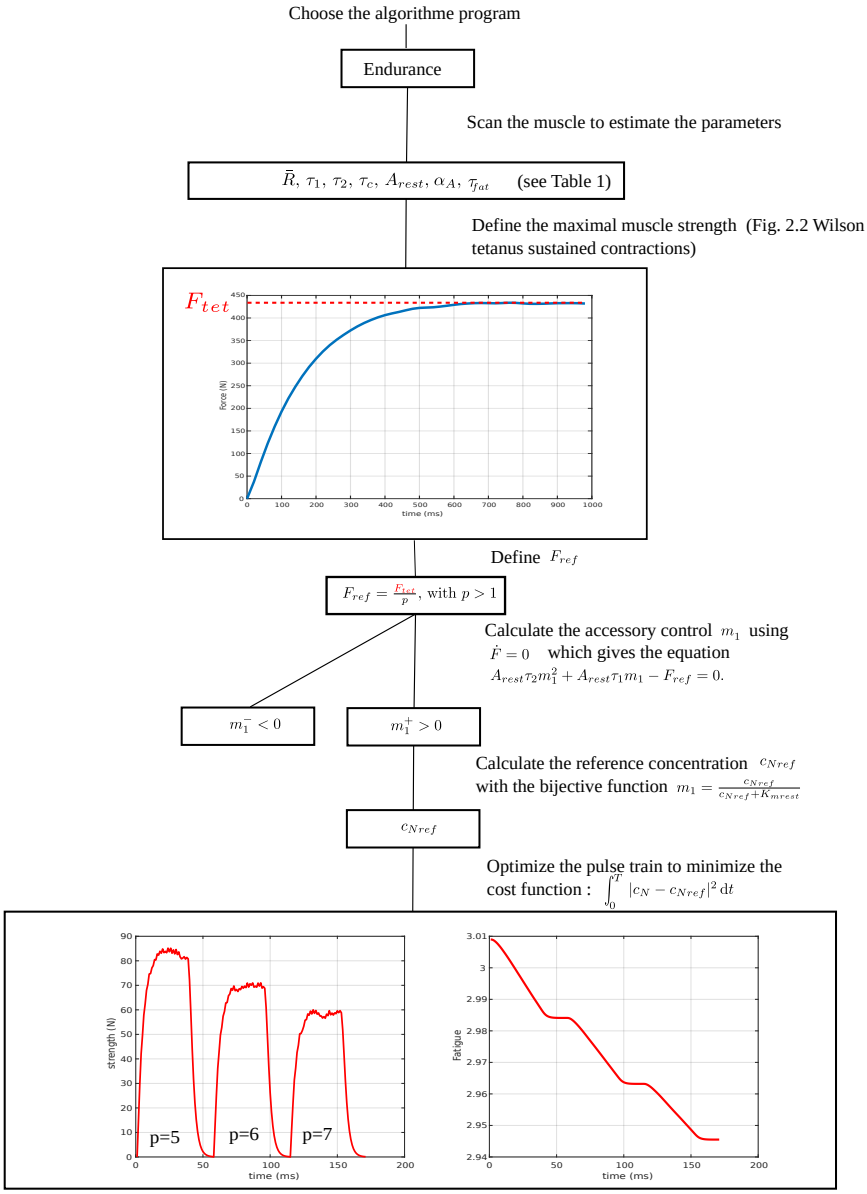

Fig. 6. Endurance program for a smart electrostimulator.

6.2 The non-isometric case

In the non-isometric case, from [Bonnard & Rouot, 2020] the force response F is coupled to a joint angular variable denoted θ to force a nonlinear pendulum with dynamics of the form :

$$\ddot{\theta}(t) + a\,\cos(\theta(t)) = F(t), \tag{31}$$

where a is a scaling parameter. Note that the output tracking problem using the output θ can be analyzed as previously in Section 6.1, to make the control appears by successive derivation of θ. We propose an alternative approach.

The first step is to choose in the θ-variable a parameterized path $L : t \mapsto \theta_d(t)$ joining two points A and B,

$t \in J = (0, t_f)$ being subdivised into intervals $J_k = (t_k, t_{k+1})$.

On each such subinterval, one can approximate $t \mapsto \theta_d(t)$ by a solution of (31) with initial conditions given by $\theta(t_k) = \theta_d(t_k)$, $\dot\theta(t_k) = \dot\theta_d(t_k)$, where F =constant on (t_k, t_{k+1}) is chosen so that to minimize some criterion or imposing $\theta(t_{k+1}) = \theta_d(t_{k+1})$.

This gives a geometric interpolation of the reference curve, defining on each subinterval a constant reference F^k_{ref}. It can be taken as a reference force, to be tracked by the concentration c_N, using sampled-data control, as in Section 6.1.

Note that $F = F_{ref}$, the equation (31) can be integrated as follows to give the explicit form of the approximated path. Indeed, it can be written as:

$$\frac{\mathrm{d}}{\mathrm{d}t}\Big(\ddot\theta(t) + V(\theta(t))\Big) = 0, \tag{32}$$

where $V(\theta) = a\,\sin(\theta) - F_{ref}\theta$ is the (forced) potential. Integrating this leads to :

$$\dot\theta^2(t) + V(\theta(t)) = E, \tag{33}$$

where E is a constant. This leads to compute $\theta(t)$, by inverting the function defined by $\int_0^{\theta(t)} \frac{\mathrm{d}\theta}{\sqrt{E - V(\theta)}} = t$.

7 Conclusion

In this short article, we have mainly presented a finite dimensional approximation of the muscular force response to FES-input. The construction is based on the Ding et al. model but can be adapted to deal with the different models discussed in [Wilson, 2011]. We have presented two toys applications of our study related to motion planning in the isometric case and the non-isometric case. Our approximation can be used to parameters estimation [Wilson, 2011,Stein *et al.*, 2013] and to design MPC-optimized sampled-data control schemes, applying standard algorithms [Richalet, 1993,Wang & Boyd, 2010] to this situation.

References

[Bakir *et al.*, 2019] Bakir T., Bonnard B. & Rouot J. (2019). A case study of optimal input-output system with sampled-data control: Ding et al. force and fatigue muscular control model. *Netw. Hetero. Media*, **14**(1), 79–100.

[Bakir *et al.*, 2020] Bakir T., Bonnard B., Bourdin L. & Rouot J. (2020). Pontryagin-type conditions for optimal muscular force response to functional electrical stimulations. *J. Optim. Theory Appl.*, **184**, 581–602.

[Bonnard & Rouot, 2020] Bonnard B. & Rouot J. (2020). Geometric optimal techniques to control the muscular force response to functional electrical stimulation using a non-isometric force-fatigue model. *Journal of Geometric Mechanics, American Institute of Mathematical Sciences (AIMS).*

[Bourdin & Trélat, 2016] Bourdin L. & Trélat E. (2016). Optimal sampled-data control, and generalizations on time scales. *Math. Cont. Related Fields*, **6**, 53–94.

[Boyd & Vandenberghe, 2004] Boyd S. & Vandenberghe L. (2004). Convex Optimization. *Cambridge, U.K.: Cambridge Univ. Press.*

[Doll *et al.*, 2015] Doll B.D. , Kirsch N.A. & Sharma N. (2015). Optimization of a Stimulation Train based on a Predictive Model of Muscle Force and Fatigue. *IFAC-PapersOnLine*, **48**(20), 338–342.

[Ding *et al.*, 2000] Ding J., Wexler A.S. & Binder-Macleod S.A. (2000). Development of a mathematical model that predicts optimal muscle activation patterns by using brief trains. *J. Appl. Physiol.*, **88**, 917–925.

[Ding *et al.*, 2002a] Ding J., Wexler A.S. & Binder-Macleod S.A. (2002). A predictive fatigue model. I. Predicting the effect of stimulation frequency and pattern on fatigue. IEEE Transactions on Neural Systems and Rehabilitation Engineering, **10**(1), 48–58.

[Ding *et al.*, 2002b] J. Ding, A.S. Wexler & S.A. Binder-Macleod, A predictive fatigue model. II. Predicting the effect of resting times on fatigue. IEEE Transactions on Neural Systems and Rehabilitation Engineering, **10** no.1 (2002), 59–67.

[Gesztelyi *et al.*, 2012] R. Gesztelyi, J. Zsuga, A. Kemeny-Beke, B. Varga, B. Juhasz & A. Tosaki, The Hill equation and the origin of quantitative pharmacology. *Archive for history of exact sciences*, **66** no. 4 (2012), 427–438.

[Hirschorn & Davis, 1987] Hirschorn, R. M. & Davis, J. H., Output tracking for nonlinear systems with singular points. SIAM J. Control Optim. 25 (1987), no. 3, 547–557.

[Hirschorn & Davis, 1988] Hirschorn, R. M. & Davis, J. H., Global output tracking for nonlinear systems. SIAM J. Control Optim. 26 (1988), no. 6, 1321–1330.

[Isidori, 1989] Isidori A. (1995). Nonlinear Control Systems. *3rd ed. Berlin, Germany: Springer-Verlag.*

[Gesztelyi *et al.*, 2012] Marion M.S., Wexler A.S. & Hull M.L. (2013). Predicting non-isometric fatigue induced by electrical stimulation pulse trains as a function of pulse duration. *Journal of neuroengineering and rehabilitation*, **10**(1).

[Michaelis & Menten, 1913] Michaelis L. & Menten M.L. (1913). Die Kinetik der Intertinwerkung. *Biochemische Zeitschrift*, **49** 333-369.

[Richalet, 1993] Richalet J. (1993). Industrial applications of model based predictive control. *Automatica, IFAC* **29**(5), 1251–1274.

[Stein *et al.*, 2013] Stein R., Bucci V., Toussaint N.C., Buffie C.G., Rätsch G., Pamer E.G. et al. (2013). = Ecological Modeling from Time-Series Inference: Insight into Dynamics and Stability of Intestinal Microbiota. *PLOS Computational Biology* **9**(12), 1–11.

[Wang & Boyd, 2010] Wang Y. & Boyd S. (2010). Fast Model Predictive Control using Online Optimization. *Control Systems Technology, IEEE Transactions on,* **18**(2), 267–278.

[Wilson, 2011] Wilson E. (2011). Force response of locust skeletal muscle. Southampton University, Ph.D. thesis.

A Appendix: Ding et al. model parameters

Table A.1
List of variables and values of the constant parameters in the Ding et al. model

Symbol	Unit	Value	Description
C_N	—	—	Normalized amount of Ca^{2+}-troponin complex
F	mN	—	Force generated by muscle
t_i	s	—	Time of the i^{th} pulse
n	—	—	Total number of the pulses before time t
i	—	—	Stimulation pulse index
τ_c	s	0.02	Time constant that commands the rise and the decay of C_N
R	—	1.143	Term of the enhancement in C_N from successive stimuli
A	$\frac{\text{mN}}{s}$	—	Scaling factor for the force and the shortening velocity of muscle
τ_1	s	—	Force decline time constant when strongly bound cross-bridges absent
τ_2	s	0.1244	Force decline time constant due to friction between actin and myosin
K_m	—	—	Sensitivity of strongly bound cross-bridges to C_N
A_{rest}	$\frac{\text{mN}}{s}$	3.009	Value of the parameter A when muscle is not fatigued
α_A	$\frac{1}{s^2}$	$-4.0\ 10^{-1}$	Coefficient for the force-model parameter A in the fatigue model
τ_{fat}	s	127	Time constant controlling the recovery of ($A,\ K_m,\ \tau_1$)